The missing aerosol response in twentieth-century mid-latitude precipitation observations

Table S1: CMIP5 models used in the analysis and the ensemble size of the historical (all forcings) experiment

Model	Ensemble size
ACCESS1-0	1
bcc-csm1-1	3
CanESM2	5
CCSM4	6
CNRM-CM5	10
CSIRO-Mk3-6-0	10
FGOALS-s2	1
GFDL-CM3	5
GFDL-ESM2G	1
GFDL-ESM2M	1
GISS-E2-H	5
GISS-E2-R	5
HadGEM2-ES	4
inmcm4	1
IPSL-CM5A-LR	5
IPSL-CM5A-MR	3
IPSL-CM5B-LR	1
MIROC5	4
MIROC-ESM	3
MPI-ESM-LR	3
MPI-ESM-P	2
MRI-CGCM3	3
NorESM1-M	3

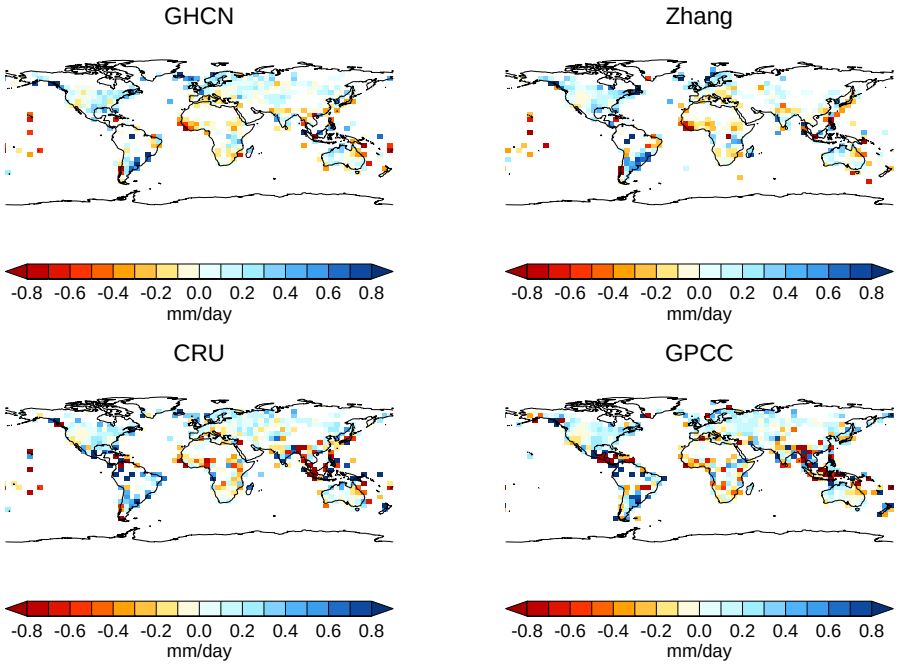

Figure S1: Land precipitation change between 1905-1924 and 1985-2004 (mm/day) for the GHCN, Zhang, CRU and GPCC datasets (Methods). Only grid-boxes where data exists for at least 50% of months in each twenty-year period are considered.

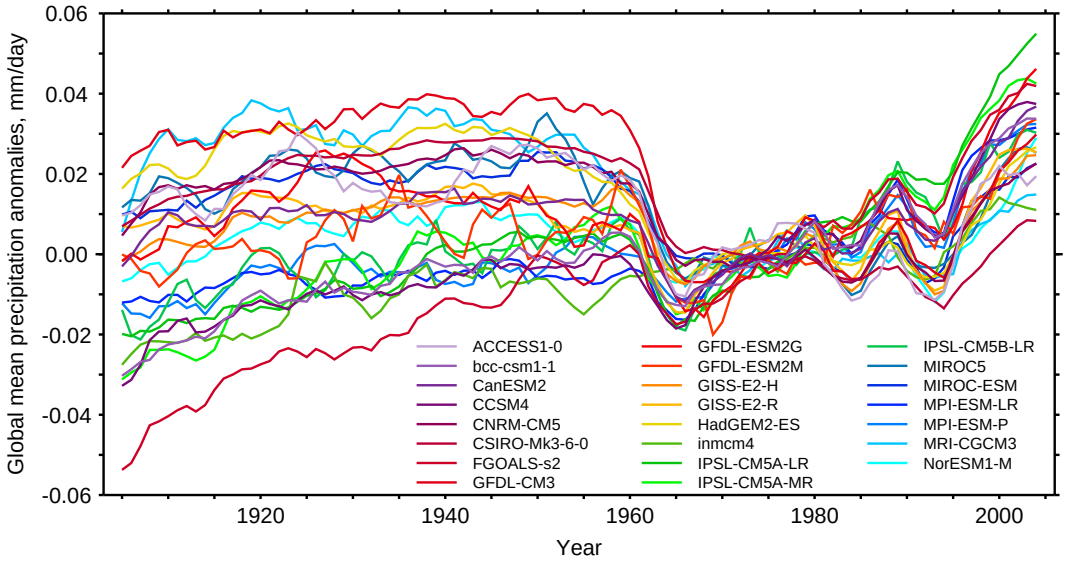

Figure S2: Global mean precipitation anomalies. Data are from 23 CMIP5 models (Supplementary Table S1). All data are for 1905-2004 and are anomalised with respect to the period 1961-1990.

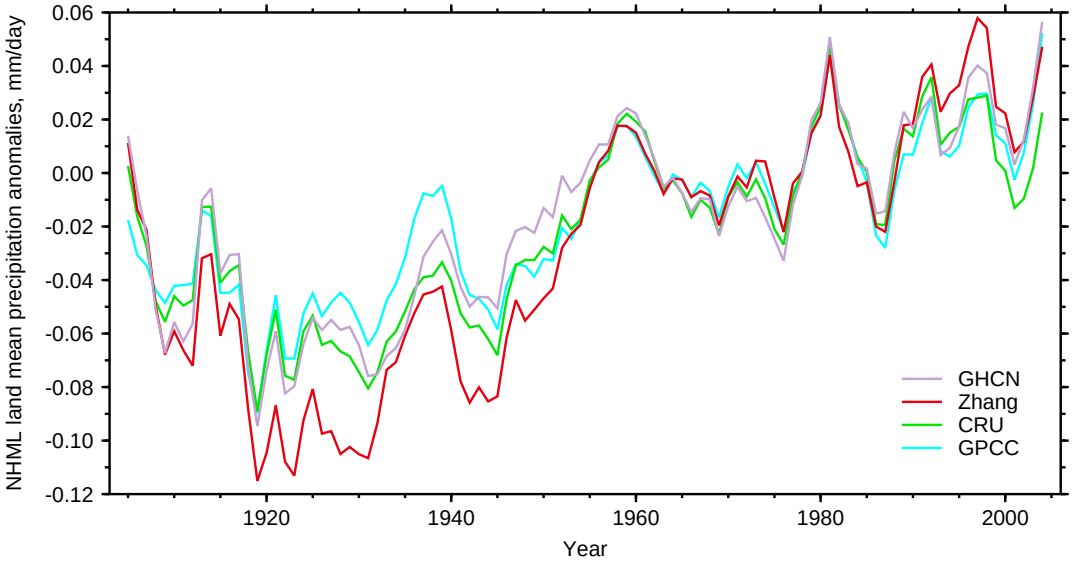

Figure S3: NHML land mean precipitation anomalies. Data are from four gridded observational datasets (Methods). All data are for 1905-2004 and are anomalised with respect to the period 1961-1990.

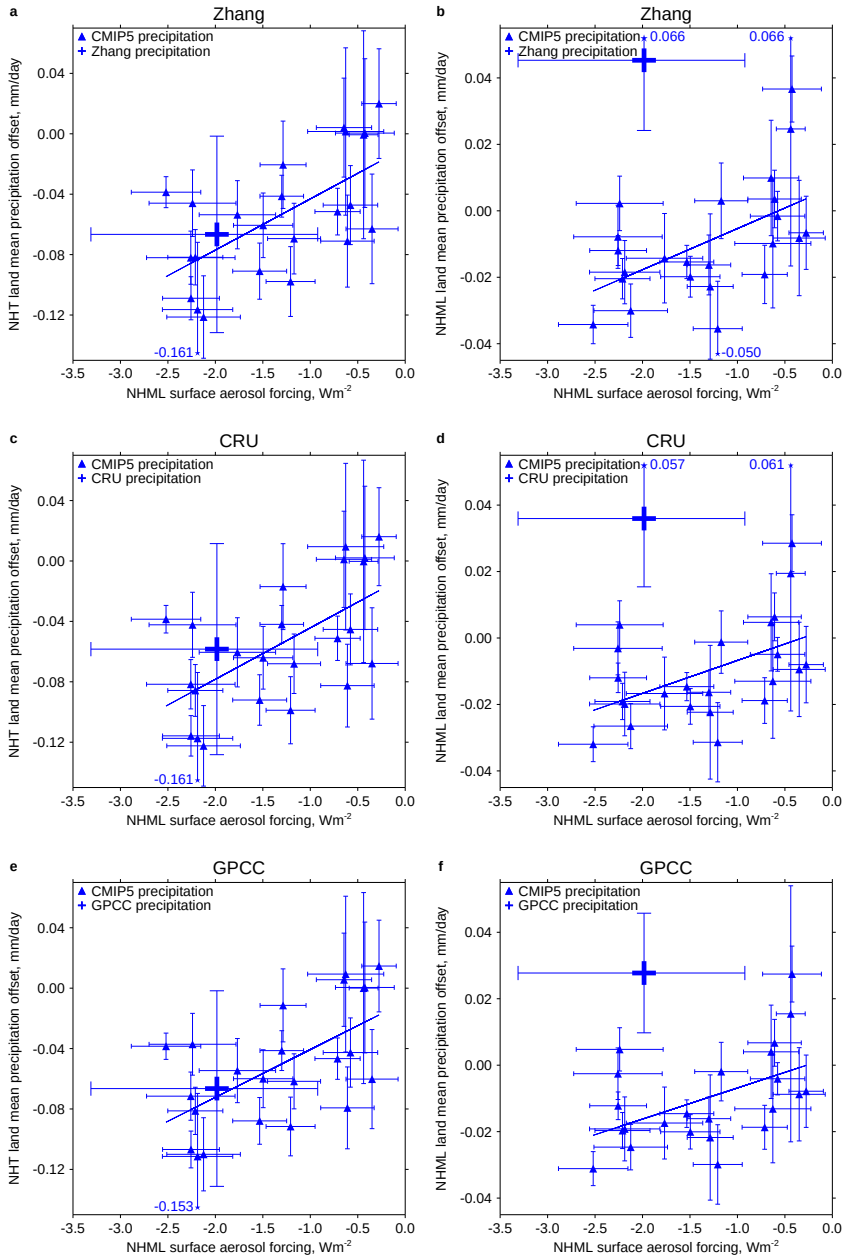

Figure S4: NHT land mean (left column) and NHML land mean (right column) precipitation offsets against NHML surface aerosol forcing using masks from the Zhang (top row), CRU (middle row) and GPCC (bottom row) datasets. Error bars represent the 5-95% uncertainty range (Methods), with IPCC equivalent NHML surface aerosol forcing and the associated 5-95% uncertainty range used for the observed data points (Supplementary Note and Supplementary Fig. S5). The proximity of the observed data points to the regression lines can be seen as indicative of the level of agreement between observations and models. The values next to the error bars are where uncertainties extend beyond the scale.

Supplementary Note

Calculating an IPCC equivalent NHML surface aerosol forcing

We use a two-step approach to calculate an IPCC equivalent NHML surface aerosol forcing for the observed temperature and precipitation offsets. Firstly, a technique similar to the IPCC approach for calculating present-day global mean TOA aerosol forcing is implemented. Then, through determining the global mean TOA aerosol forcing relationship with NHML surface aerosol forcing (Supplementary Fig. S5) across the CMIP5 models, we calculate an IPCC equivalent NHML surface aerosol forcing for the observed offsets.

The latest IPCC[1] present-day global mean aerosol forcing estimate is -0.9 (5-95% uncertainty range of -1.9 to -0.1) Wm^{-2}. Our approach to calculating global mean TOA aerosol forcing for individual CMIP5 models is analogous to the effective radiative forcing concept used in the IPCC Fifth Assessment Report (AR5)[1], except that we use a simple linear forcing-feedback model approach (Methods), rather than a fixed-SST technique, although differences in the two types of forcing estimate have been shown to be small[2]. The IPCC estimate is for 2011 relative to 1750. Here, we take the 2002-2004 mean forcing relative to a pre-industrial control simulation. The main difference in these values is expected to come from our use of SW forcing to represent total aerosol forcing (Methods and Supplementary Fig. S8). However, we expect our technique to still be representative of the relative strength of present-day aerosol forcing in the CMIP5 models.

Our IPCC-style global mean TOA aerosol forcing estimate is strongly correlated ($r=0.70$, $p<0.01$) with NHML TOA aerosol forcing, which is calculated using the approach detailed in the Methods section, excluding the MRI-CGCM3 and CNRM-CM5 models. Considering the spatial pattern of SW forcing (not shown) in MRI-CGCM3, we identify strong aerosol forcing in the tropics, but weak aerosol forcing in the NHML region, contrary to output from other models and our scientific understanding of twentieth-century aerosol forcing[3]. This model is retained in the main analysis considering the offset-aerosol forcing relationship, because both the mean temperature gradient response and NHML land mean precipitation response are in keeping with weak NHML aerosol forcing. We might expect this unusual spatial pattern of SW forcing to affect the NHT land mean precipitation response, but find no evidence for this, consistent with other work, which suggests that tropical precipitation is more sensitive to remote aerosol forcing than local aerosol forcing[4]. Further, this would suggest that NHML land mean precipitation appears insensitive to remote tropical aerosol forcing, at least in the MRI-CGCM3 model. Using the relationship across CMIP5 models (without MRI-CGCM3 and CNRM-CM5) IPCC equivalent NHML TOA aerosol forcing is -1.7 (-2.9 to -0.7) Wm^{-2}.

NHML TOA aerosol forcing is very strongly correlated ($r=0.97$, $p<0.01$) with NHML

surface aerosol forcing, again calculated using the approach detailed in the Methods section (Supplementary Fig. S5). Despite very strong NHML surface aerosol forcing, the CNRM-CM5 model has weak NHML TOA aerosol forcing, so is excluded here. This is perhaps indicative of black carbon, a strongly absorbing aerosol at SW wavelengths. Again, this model is included in the main analysis, because significant black carbon forcing would be expected to produce strongly negative NHML surface aerosol forcing and an even greater negative precipitation offset in the mid-twentieth century. IPCC equivalent NHML surface aerosol forcing is calculated as -2.0 (-3.3 to -0.9) Wm^{-2}.

The aerosol estimate in AR5 originates from a more detailed methodology than that presented here, incorporating, for example, global chemistry modelling and (in-situ and remote) observations. Our technique is trained on the forcing seen in CMIP5 models. As such, our method provides a largely independent estimate of real-world present-day aerosol forcing to that presented in AR5.

Removing the abrupt mean temperature gradient shift

In agreement with previous work[5], we find an abrupt decrease in the observed mean temperature gradient that is centred around 1970. This shift has been attributed to internal variability and is seemingly not captured by CMIP5 models[6]. We investigate whether a temperature gradient offset in response to aerosol forcing is still evident once the abrupt shift has been removed. The difference between the 1963-67 and 1973-77 mean temperature gradient means (0.36 K) is taken as the magnitude of the late 1960s shift. Increasing all 1968-2004 annual anomalies by this value, we calculate a new offset (Methods) for the mean temperature gradient with this abrupt shift removed.

This simple technique gives a mean temperature gradient offset that is in better agreement with what might be expected from real-world NHML surface aerosol forcing. However, it is also possible that part of the observed NHT land mean precipitation offset is attributable to this sudden shift in the mean temperature gradient. While this might influence the robust relationship between the observed NHT land mean precipitation offset and IPCC equivalent NHML surface aerosol forcing, we again note that a strong link between mid-twentieth-century aerosol forcing (primarily remote forcing from the NHML region) and a southward tropical precipitation shift (comparable to decreasing NHT land mean precipitation) has been found in other studies[7-8]. While a robust feature, the southward precipitation shift - defined using a different measure - has actually been found to be underestimated in CMIP5 models[8]. Further, it has been suggested that aerosol emissions may be the dominant influence on North Atlantic ocean variability[9], which is frequently identified as the key contributor to the abrupt mean temperature gradient shift, casting some doubt on whether this is simply an internal variability-driven signal.

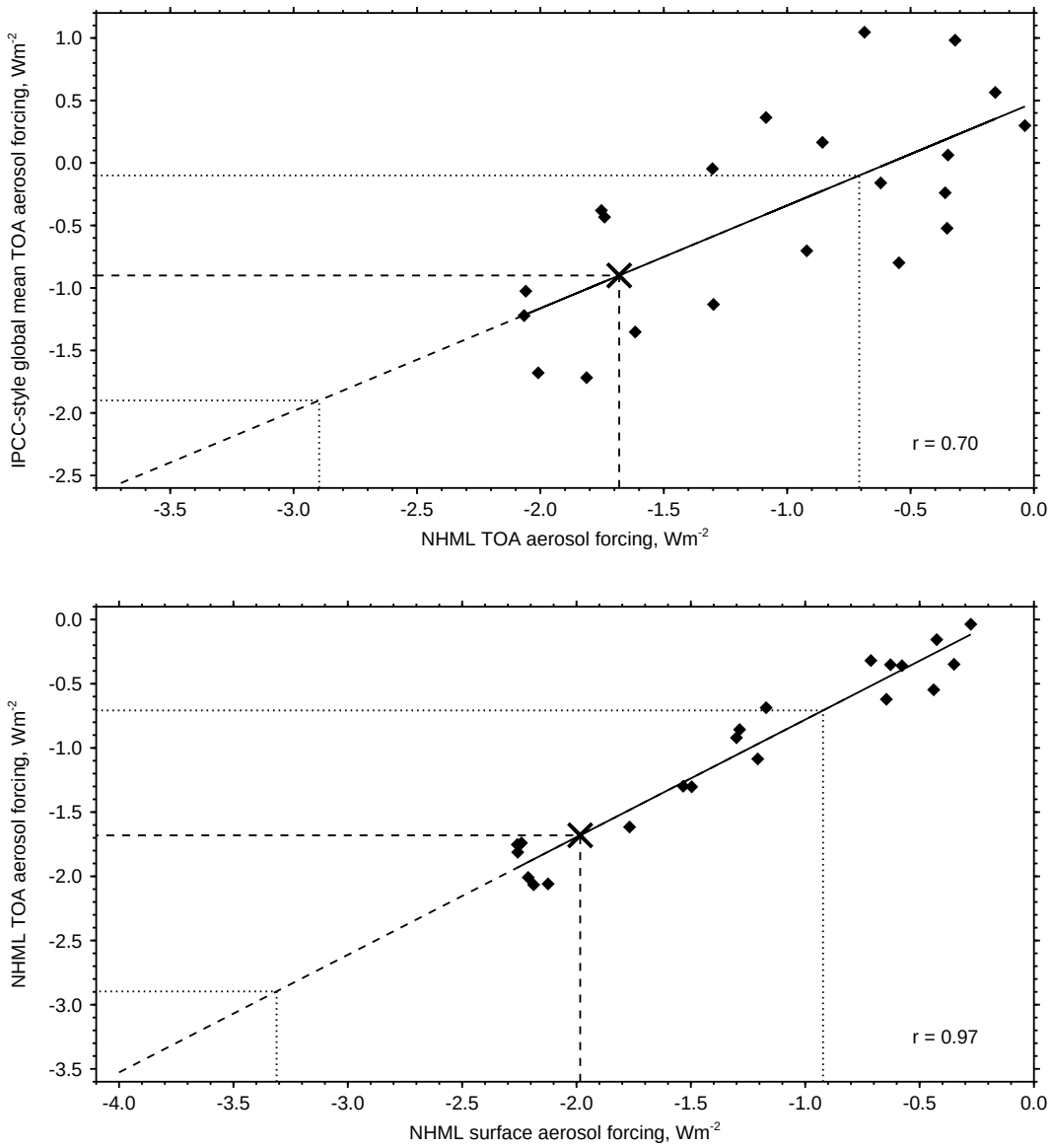

Figure S5: IPCC-style global mean TOA aerosol forcing against NHML TOA aerosol forcing (top panel) and NHML TOA aerosol forcing against NHML surface aerosol forcing (bottom panel) for 21 CMIP5 models (Supplementary Note). Using linear regression the IPCC equivalent NHML TOA aerosol forcing (cross and dashed lines) and 5-95% uncertainty range (dotted lines) are shown given the IPCC AR5 present-day global mean aerosol forcing estimate and uncertainty range (top panel). The process is repeated to show IPCC equivalent NHML surface aerosol forcing given IPCC equivalent NHML TOA aerosol forcing (bottom panel). Correlation coefficients, r, are shown.

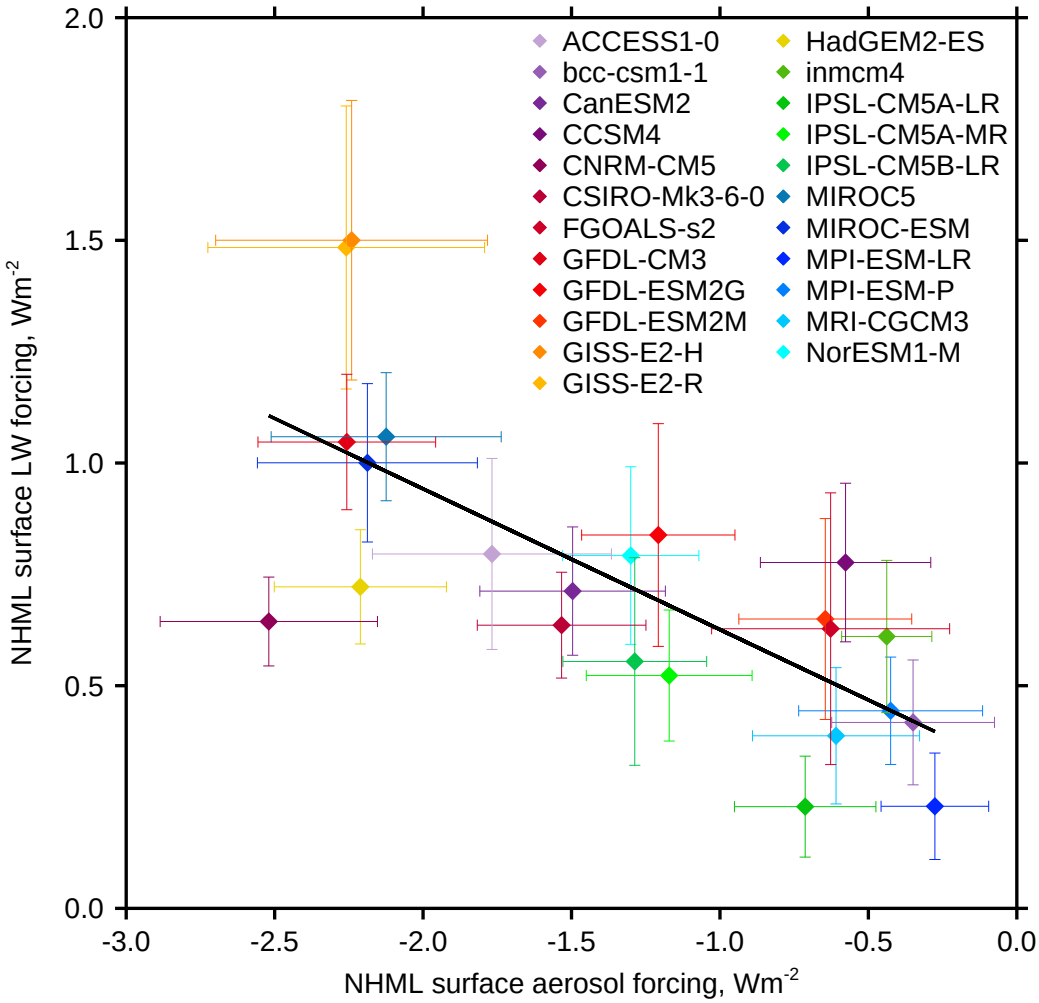

Figure S6: NHML surface LW forcing against NHML surface aerosol forcing for 23 CMIP5 models. NHML surface LW forcing is calculated using the technique outlined in Methods, replacing surface SW fluxes with surface LW fluxes and taking the difference between mean NHML mean surface LW forcing before and after 1960. Horizontal and vertical error bars show an estimate of the 5-95% uncertainty ranges in NHML surface aerosol forcing and NHML surface LW forcing respectively. Surface LW and surface aerosol forcing are clearly anti-correlated in the NHML region ($r=-0.72$, $p<0.01$), but the GISS-E2-H and GISS-E2-R climate models have anomalously strong NHML surface LW forcing. Because of this large increase in NHML surface LW forcing in the mid-twentieth-century, these models do not show the interhemispheric forcing asymmetry expected from their level of NHML surface aerosol forcing. In turn, both the mean temperature gradient and the NHT land mean precipitation offsets will not be as great as implied by NHML surface aerosol forcing alone. Likewise, the NHML land mean precipitation offsets are underestimated, as SW-induced surface cooling is counteracted by significant LW-induced surface warming.

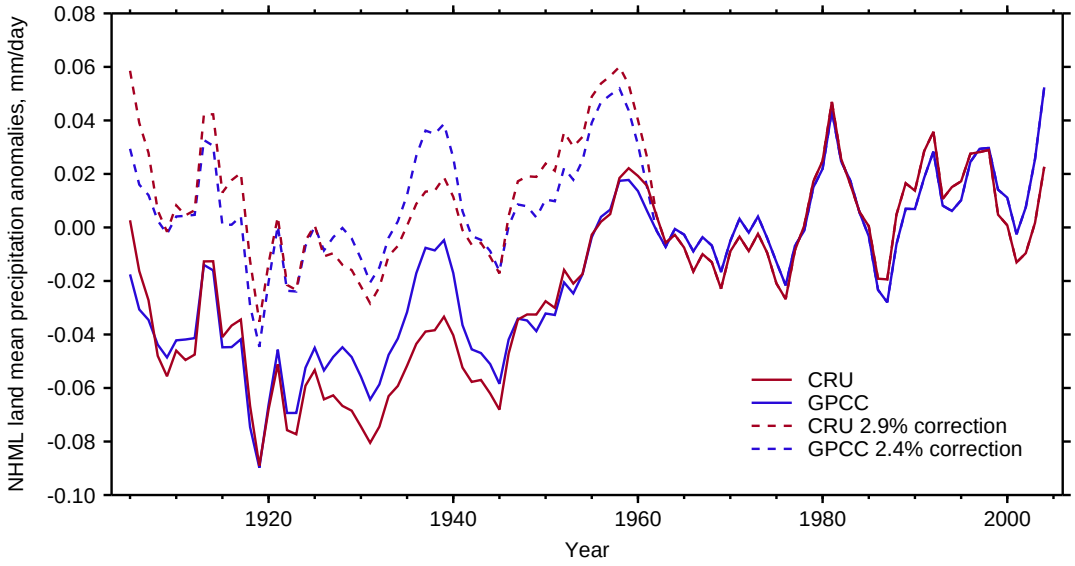

Figure S7: NHML land mean precipitation anomalies for the CRU and GPCC datasets. Corrected data, where monthly total precipitation prior to 1960 is increased by 2.9% and 2.4% for CRU and GPCC respectively are shown (dashed lines). The NHML land precipitation offsets (Methods) for the corrected data are consistent with IPCC equivalent NHML surface aerosol forcing and, in turn, the temperature gradient offsets and the NHT land precipitation offsets. All data are for 1905-2004 and are anomalised with respect to the period 1961-1990.

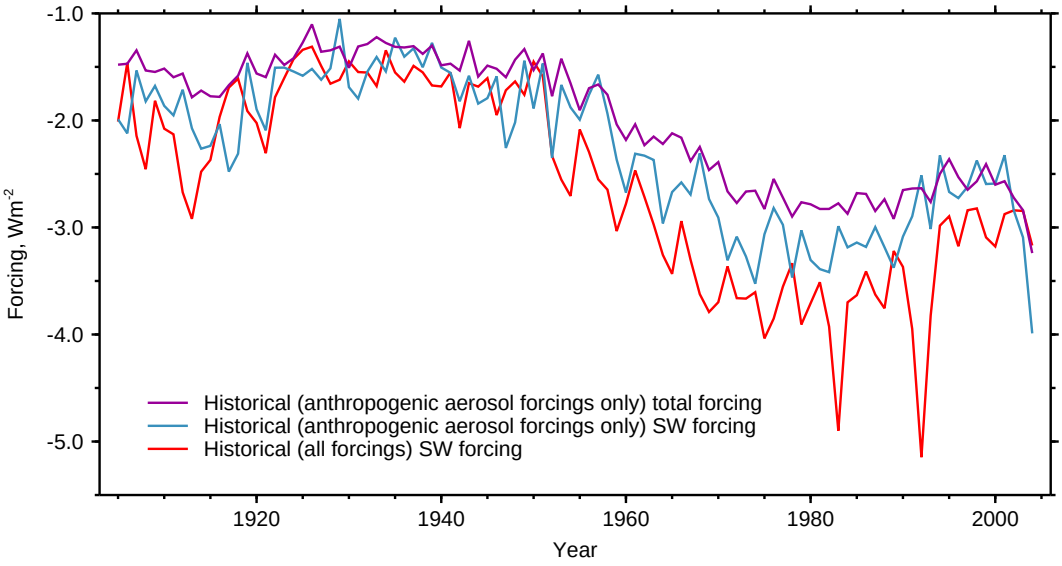

Figure S8: Time series of NHML surface total forcing and NHML surface SW forcing from the historical anthropogenic aerosol forcings only experiment and of NHML surface SW forcing from the historical all forcings experiment for the CSIRO-Mk3-6-0 model for 1905-2004. Forcing is given relative to a pre-industrial control simulation.

References

1. Myhre, G. *et al.* in *Climate Change 2013: The Physical Science Basis. Contribution of Working Group I to the Fifth Assessment Report of the Intergovernmental Panel on Climate Change* (eds Stocker, T. F. *et al.*) Ch. 8 (Cambridge Univ. Press, 2013)

2. Andrews, T., Gregory, J. M., Webb, M. J. & Taylor, K. E. Forcing, feedbacks and climate sensitivity in CMIP5 coupled atmosphere-ocean climate models. *Geophys. Res. Lett.* **39,** L09712 (2012).

3. Lamarque, J. F. *et al.* Historical (1850-2000) gridded anthropogenic and biomass burning emissions of reactive gases and aerosols: Methodology and application. *Atmos. Chem. Phys.* **10,** 7017-7039 (2010).

4. Shindell, D. T., Voulgarakis, A., Faluvegi, G. & Milly, G. Precipitation response to regional radiative forcing. *Atmos. Chem. Phys.* **12,** 6969-6982 (2012).

5. Thompson, D. W. J., Wallace, J. M., Kennedy, J. J. & Jones, P. D. An abrupt drop in Northern Hemisphere sea surface temperature around 1970. *Nature* **467,** 444-447 (2010).

6. Friedman, A. R., Hwang, Y-T., Chiang, J. C. H. & Frierson, D. M. W. Interhemispheric temperature asymmetry over the twentieth century and in future projections. *J. Clim.* **26,** 5419-5433 (2013).

7. Chang, C-Y., Chiang, J. C. H., Wehner, M. F., Friedman, A. R. & Ruedy, R. Sulfate aerosol control of tropical Atlantic climate over the twentieth century. *J. Clim.* **24,** 2540-2555 (2011).

8. Hwang, Y-T., Frierson, D. M. W. & Kang, S. M. Anthropogenic sulphate aerosol and the southward shift of tropical precipitation in the late 20th century. *Geophys. Res. Lett.* **40,** 2845-2850 (2013).

9. Booth, B. B. B. *et al.* Aerosols implicated as a prime driver of twentieth-century North Atlantic climate variability. *Nature* **484,** 228-232 (2012).